

# Cu hyperfine coupling constants of $\text{HgBa}_2\text{CaCu}_2\text{O}_{6+\delta}$

Yutaka Itoh<sup>1</sup>, Takato Machi<sup>2</sup> and Ayako Yamamoto<sup>3</sup>

<sup>1</sup>Department of Physics, Graduate School of Science, Kyoto Sangyo University,  
Kamigamo-Motoyama, Kika-ku, Kyoto 603-8555, Japan

<sup>2</sup>AIST Tsukuba East, Research Institute for Energy Conservation, 1-2-1 Namiki, Tsukuba,  
Ibaraki 305-8564, Japan

<sup>3</sup>Graduate School of Engineering and Science, Shibaura Institute of Technology, 3-7-5 Toyosu,  
Koto-ku, Tokyo 135-8548, Japan

E-mail: yitoh@cc.kyoto-su.ac.jp

**Abstract.** We estimated the ratios of  $^{63}\text{Cu}$  hyperfine coupling constants in the double-layer high- $T_c$  superconductor  $\text{HgBa}_2\text{CaCu}_2\text{O}_{6+\delta}$  from the anisotropies in Cu nuclear spin-lattice relaxation rates and spin Knight shifts to study the nature of the ultraslow fluctuations causing the  $T_2$  anomaly in the Cu nuclear spin-echo decay. The ultraslow fluctuations may come from uniform magnetic fluctuations spread around the wave vector  $q = 0$ , otherwise the electric origins.

## 1. Introduction

Spin polarized neutron scattering experiments indicate the emergence of an intra-unit-cell (IUC)  $q = 0$  magnetic moments in the pseudogap states of the high- $T_c$  cuprate superconductors, while no NMR and  $\mu\text{SR}$  experiment indicates any static ordering of local magnetic moments [1]. The IUC moments are associated with the loop current ordered state [2]. Recently discovered ultraslow fluctuations in the pseudogap states of  $\text{HgBa}_2\text{CaCu}_2\text{O}_{6+\delta}$  (Hg1212) via  $^{63}\text{Cu}$  nuclear spin-echo decay experiments [3] might reconcile an issue on the IUC moments. No wipeout effect on NMR spectra is characteristic of the ultraslow fluctuations of Hg1212, in contrast to the spin-charge stripe orderings [4, 5].

Knowledge of the hyperfine coupling constants helps us to clarify the nature of the local field fluctuations in NMR measurements [6]. In this paper, we report the estimation of the  $^{63}\text{Cu}$  hyperfine coupling constants in the double- $\text{CuO}_2$ -layer high- $T_c$  superconductors Hg1212 from the anisotropies in  $^{63}\text{Cu}$  nuclear spin-lattice relaxation rates and spin Knight shifts [7], and discuss the nature of the ultraslow fluctuations [3].

## 2. Estimations of $^{63}\text{Cu}$ hyperfine coupling constants

The  $^{63}\text{Cu}$  hyperfine coupling parameters ( $A_{cc}^{hf}$  and  $A_{ab}^{hf}$ ) consist of the anisotropic on-site  $A_{cc}$  (the  $c$  axis component) and  $A_{ab}$  (the  $ab$  plane component) due to the  $3d$  electrons and the isotropic supertransferred component  $B(> 0)$  [6]. The ratios of the individual components in the three coupling constants can be estimated from the anisotropy data [7] of the  $^{63}\text{Cu}$  Knight shifts ( $^{63}K_{cc}$  and  $^{63}K_{ab}$ ) and the  $^{63}\text{Cu}$  nuclear spin-lattice relaxation rates  $[(1/T_1)_{cc}$  and  $(1/T_1)_{ab}]$  via the antiferromagnetic dynamical spin susceptibility [6, 8, 9, 10, 11]. The subscript indices

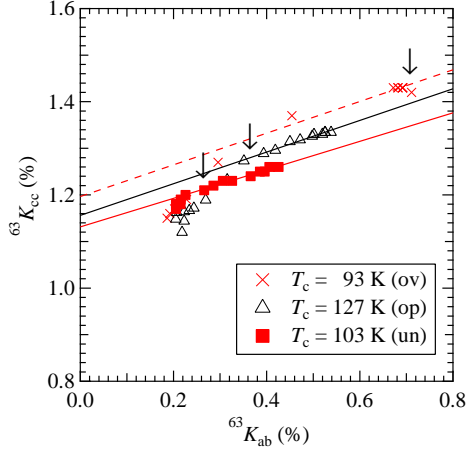


**Figure 1.**  $^{63}K_{cc}$  versus  $^{63}K_{ab}$  with temperature as an implicit parameter for Hg1212 from underdoped to overdoped [7]. The arrows indicate  $T_c$ .

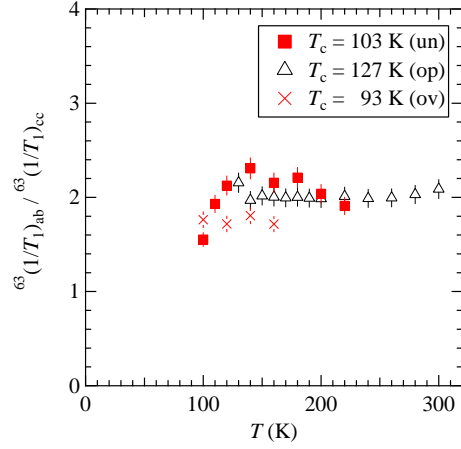


**Figure 2.** Anisotropy ratio  $^{63}(1/T_1)_{ab}/^{63}(1/T_1)_{cc}$  against temperature for Hg1212 from underdoped to overdoped [7].

of  $cc$  or  $ab$  of  $^{63}K$  and  $1/T_1$  indicate the direction of a static magnetic field applied along the  $c$  axis or in the  $ab$  plane. The procedure to estimate the coupling constant ratios is shown below.

### 2.1. $^{63}Cu$ Knight shifts

The  $^{63}Cu$  Knight shifts  $^{63}K_{cc,ab}$  at a magnetic field along the  $c$  axis or in the  $ab$  plane are the sum of the spin shift  $K_{spin}$  and the orbital shift  $K_{orb}$  as  $^{63}K_{cc,ab} = K_{spin}^{cc,ab}(T) + K_{orb}^{cc,ab}$ . The spin shift is  $K_{spin}^{cc,ab}(T) = A_{cc,ab}^{hf} \chi_s^{cc,ab}(T)$  with the hyperfine coupling parameters  $A_{cc,ab}^{hf}$  and the uniform spin susceptibility  $\chi_s^{cc,ab}(T)$ . For a temperature-dependent isotropic spin susceptibility  $\chi_s^{cc} = \chi_s^{ab}$ , the ratio  $\Delta K_{spin}^{cc}/\Delta K_{spin}^{ab} = (dK_{spin}^{cc}/dT)/(dK_{spin}^{ab}/dT)$  is equal to the ratio  $A_{cc}^{hf}/A_{ab}^{hf}$ .

Figure 1 shows  $^{63}K_{cc}$  plotted against  $^{63}K_{ab}$  with temperature as an implicit parameter for Hg1212 from underdoped to overdoped, which are adopted from [7]. The solid straight lines are the least-squares fitting results. The dashed straight line for overdoped Hg1212 is a visual guide with assuming the same slope as the optimally doped Hg1212. The straight lines show nearly parallel shift. Since the orbital shifts of  $K_{orb}^{cc} = 1.14\text{--}1.16\%$  and  $K_{orb}^{ab} = 0.19\text{--}0.20\%$  are estimated below  $T_c$ , then the parallel shift indicates a constant spin component above  $T_c$ . Similar parallel shift is found in the single crystal NMR for  $HgBa_2CuO_{4+\delta}$  [12].

An easy plane magnetic anisotropy causes such a constant spin component in the paramagnetic spin susceptibility [13]. The anisotropic superexchange interaction in the  $S = 1/2$  XXZ Heisenberg Hamiltonian yields the easy plane anisotropy in the paramagnetic state [14, 15]. The optimally hole doping makes the anisotropy weak [13, 16]. Although the multicomponents in the spin susceptibility are suggested from the anisotropic spin Knight shifts [12, 17], we believe that the doped superconductors with a single spin component can show a finite anisotropy and that the constant spin component does not impede a single spin component analysis to estimate the Cu hyperfine coupling constants.

The  $^{63}Cu$  hyperfine coupling parameters  $A_{cc}^{hf}$  and  $A_{ab}^{hf}$  are expressed by  $A_{cc}$ ,  $A_{ab}$ , and  $B$  as  $A_{cc}^{hf} = A_{cc} + 4B$  and  $A_{ab}^{hf} = A_{ab} + 4B$  [6, 8, 18]. Then, the anisotropy ratio  $r_u$  of the

temperature-dependent  $K_s^{cc}$  and  $K_s^{ab}$  is given by

$$r_u \equiv \frac{\Delta K_s^{cc}}{\Delta K_s^{ab}} = \frac{A_{cc} + 4B}{A_{ab} + 4B}. \quad (1)$$

Figure 1 shows  $r_u = 0.31$  for the underdoped and 0.34 for the optimally doped samples. The value of  $r_u = 0.34$  is assumed for the overdoped sample.

### 2.2. $^{63}\text{Cu}$ nuclear spin-lattice relaxation rate

Figure 2 shows the ratio of  $^{63}(1/T_1)_{ab}/^{63}(1/T_1)_{cc}$  plotted against temperature for Hg1212 from underdoped to overdoped (adopted from Ref. [7]). The anisotropy ratio  $r_{AF}$  of  $(1/T_1)_{ab}$  and  $(1/T_1)_{cc}$  is given by

$$r_{AF} \equiv \frac{(1/T_1)_{ab}}{(1/T_1)_{cc}} \approx \frac{1}{2} \left\{ 1 + \left( \frac{A_{cc} - 4B}{A_{ab} - 4B} \right)^2 \right\}, \quad (2)$$

for the leading term of the enhanced antiferromagnetic susceptibility [11]. For convenience, we introduce an alternative parameter of  $r_A = \sqrt{2r_{AF} - 1}$ . We adopted the values of  $r_{AF}$  ( $r_A$ ) = 2.3 (1.90), 2.0 (1.73), and 1.8 (1.61) from underdoped to overdoped (figure 2) to estimate the coupling constant ratios.

### 2.3. $^{63}\text{Cu}$ hyperfine coupling constant ratios

From the constraints of  $A_{cc} < 0$  [18] and  $A_{ab}/4B < 1$  on (1) and (2), we obtain the expressions of the ratios of the  $^{63}\text{Cu}$  hyperfine coupling constants,

$$\frac{A_{cc}}{4B} \approx -\frac{r_A + r_u - 2r_A r_u}{r_A - r_u}, \quad (3)$$

$$\frac{A_{ab}}{4B} \approx \frac{r_A + r_u - 2}{r_A - r_u}, \quad (4)$$

and then

$$\frac{A_{ab}}{A_{cc}} \approx -\frac{r_A + r_u - 2}{r_A + r_u - 2r_A r_u}. \quad (5)$$

Thus, (3)-(5) with a set of  $r_u$  and  $r_A$  enable us to estimate the ratios of the  $^{63}\text{Cu}$  hyperfine coupling constants.

**Table 1.** Anisotropies ( $r_u$  and  $r_{AF}$ ) of  $^{63}K_s$  and  $^{63}T_1$ , and the ratios of  $^{63}\text{Cu}$  hyperfine coupling constants ( $A_{cc}$ ,  $A_{ab}$ ,  $B$ ) for underdoped (un), optimally doped (op) and overdoped (ov) Hg1212.  $T_c$  is in kelvin. The value of  $r_u$  for overdoped Hg1212 is assumed after the optimally doped value in figure 1.

	$T_c$	$r_u$	$r_{AF}$	$A_{cc}/4B$	$A_{ab}/4B$	$A_{ab}/A_{cc}$
un	103	0.31	2.3	-0.65	+0.13	-0.20
op	127	0.34	2.0	-0.64	+0.05	-0.078
ov	93	0.34	1.8	-0.67	-0.04	+0.058

Table 1 shows the estimated ratios of  $A_{cc}/4B$ ,  $A_{ab}/4B$  and  $A_{ab}/A_{cc}$  for Hg1212 from (3)-(5) with the experimental  $r_u$  and  $r_{AF}$  in figures 1 and 2. The on-site coupling ratio  $A_{ab}/A_{cc}$  depends on the hole concentration in Hg1212.

The  $3d(x^2 - y^2)$  orbital electron of  $\text{Cu}^{2+}$  in the tetragonal crystal field produces the on-site hyperfine fields. The ratio  $A_{ab}/A_{cc}$  is expressed as

$$\frac{A_{ab}}{A_{cc}} \approx -\frac{-\kappa + \frac{2}{7} - \frac{11}{7}\gamma}{-\kappa - \frac{4}{7} - \frac{62}{7}\gamma}, \quad (6)$$

where  $\kappa(> 0)$  is the core polarization parameter,  $2/7$  and  $-4/7$  are the spin-dipole field coefficients, and  $\gamma(< 0)$  is the spin-orbit coupling parameter [9, 19, 20]. The empirical values of  $\kappa = 0.25$  and  $0.325$  were estimated for  $\text{Cu}^{2+}$  ions in the dilute copper salts [20]. The first-principles cluster calculations give  $\kappa = 0.289$  for the density functional  $< 1/r^3 >$  and  $0.455$  for the Hartree-Fock  $< 1/r^3 >$  in  $\text{La}_2\text{CuO}_4$  [21]. The value of  $\kappa = 0.41$  is found in  $\text{CuGeO}_3$  [22]. For Hg1212,  $A_{ab}/A_{cc}$  in Table 1 through (6) leads to the core polarization parameter  $\kappa = 0.265$  (un),  $0.315$  (op) and  $0.387$  (ov), assuming  $\gamma = -0.044$  [9, 19].

#### 2.4. $^{63}\text{Cu}$ hyperfine coupling constants of $\text{HgBa}_2\text{CuO}_{4+\delta}$ and Hg1212

Let us show the  $^{63}\text{Cu}$  hyperfine coupling constants of the optimally doped single- $\text{CuO}_2$ -layer superconductor  $\text{HgBa}_2\text{CuO}_{4+\delta}$  ( $T_c = 98$  K). From the uniform spin susceptibility  $\chi_s = 1.47 \times 10^{-4}$  emu/mole-f.u. [23] and the in-plane  $^{63}\text{Cu}$   $K_{spin}^{ab} = 0.48$  % [24], we estimated the in-plane  $^{63}\text{Cu}$  hyperfine coupling parameter  $A_{ab}^{hf} = A_{ab} + 4B = (N_A \mu_B / \chi_s) K_{spin}^{ab} = 182$  kOe/ $\mu_B$  for  $\text{HgBa}_2\text{CuO}_{4+\delta}$  ( $N_A$  is Avogadro's number and  $\mu_B$  is the Bohr magneton). Substituting  $r_u = 0.53$  and  $r_{AF} = 1.8$  [24] into (3)-(5) and using  $A_{ab} + 4B = 182$  kOe/ $\mu_B$ , we obtained the values of

$$A_{cc} = -65, A_{ab} = 21, \text{ and } B = 40 \text{ kOe}/\mu_B$$

for the optimally doped  $\text{HgBa}_2\text{CuO}_{4+\delta}$ .

By adopting  $A_{ab} + 4B = 182$  kOe/ $\mu_B$  for Hg1212 after  $\text{HgBa}_2\text{CuO}_{4+\delta}$ , we estimated the individual components of  $A_{cc}$ ,  $A_{ab}$ , and  $B$  (Table 2). Figure 3 shows  $A_{cc}$ ,  $A_{ab}$ , and  $B$  (Table 2) plotted against the hole concentration  $P_{sh}$  [7] for Hg1212. In Table 2 and figure 3, with increase in the hole concentration, the absolute value of the negative  $A_{cc}$  increases,  $A_{ab}$  shows a sign change, and the  $B$  term slightly increases.

The reported  $B$  term is in the range from 36 to 155 kOe/ $\mu_B$  in the other cuprate superconductors [10, 25, 26, 27, 28], assuming *a priori* the fixed values of  $A_{cc} = -170$  and  $A_{ab} = 37$  kOe/ $\mu_B$  [25, 27, 28]. The cation-cation supertransferred hyperfine field  $B$  between  $3d$  and  $4s$  orbitals depends on the strength of the  $p$ - $d$  covalent bond parameter [29]. The doping dependent  $B$  term in Table 2 indicates the development of the covalency with the hole concentration in Hg1212.

**Table 2.**  $^{63}\text{Cu}$  hyperfine coupling constants in units of kOe/ $\mu_B$  for underdoped (un), optimally doped (op) and overdoped (ov) Hg1212, assuming  $A_{ab} + 4B = 182$  kOe/ $\mu_B$ .

	$A_{cc}$	$A_{ab}$	$B$
un	-105	+21	40
op	-111	+8.7	43
ov	-127	-7.4	47

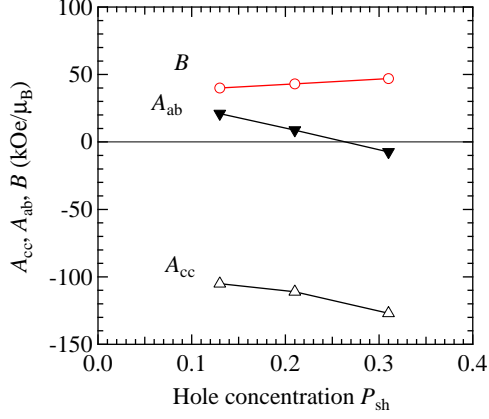


**Figure 3.**  $^{63}\text{Cu}$  hyperfine coupling constants  $A_{cc}$ ,  $A_{ab}$ , and  $B$  plotted against hole concentration  $P_{sh}$  for Hg1212. The solid curves are visual guides.

### 3. Local field fluctuations in $^{63}\text{Cu}$ nuclear spin-echo decay rate $1/T_{2L}$

#### 3.1. $^{63}\text{Cu}$ nuclear spin-echo decay rate $1/T_{2L}$

Figures 4(a)–4(c) show the  $^{63}\text{Cu}$  nuclear spin-echo decay rates  $(1/T_{2L})_{ab,cc}$ 's for Hg1212 from underdoped (a), optimally doped (b) and overdoped (c) [3]. The notations conform to those in [3]. The enhancements in  $(1/T_{2L})_{ab,cc}$  at 220–240 K indicate the ultraslow fluctuations [3]. The peak temperature of  $(1/T_{2L})_{cc}$  is nearly independent of the doping level, but the enhancement is suppressed by overdoping.

Figure 4(d) shows the anisotropy ratio of the local field fluctuations  $\Delta J_{cc}/\Delta J_{ab} \equiv [(1/T_{2L})_{cc} - (1/T_{2R})_{cc}]/[(1/T_{2L})_{ab} - (1/T_{2R})_{ab}]$  derived from  $1/T_{2L}$  and  $1/T_1$  (Redfield's  $1/T_{2R}$ ) [3].  $\Delta J_{\gamma\gamma}$  ( $\gamma\gamma = cc$  and  $ab$ ) expresses the additional fluctuations causing the enhancement in  $1/T_{2L}$ . One should note that  $\Delta J_{cc}/\Delta J_{ab} < 1$  is characteristic of the ultraslow fluctuations.

Figure 4(e) shows the phase diagram of Hg1212, where the superconducting transition temperature  $T_c$ , the pseudo spin-gap temperature defined by the maximum temperature of

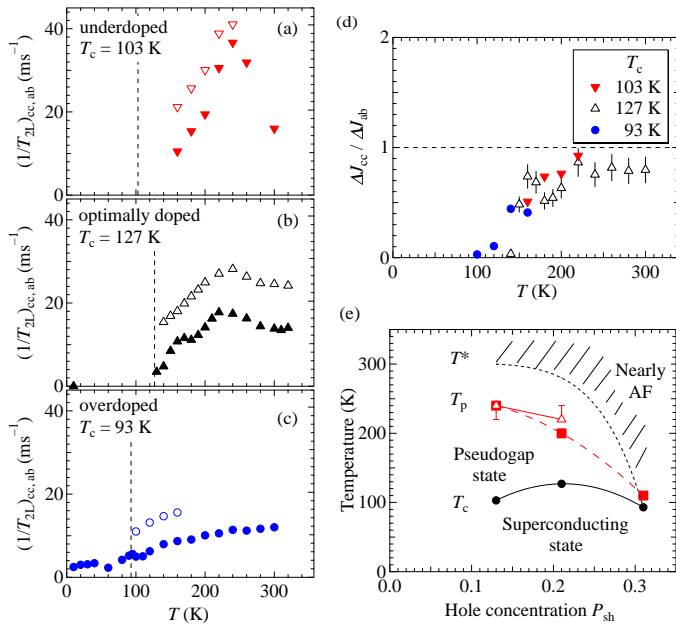


**Figure 4.** (a)–(c)  $T$  dependences of  $(1/T_{2L})_{cc}$  (closed symbols) and  $(1/T_{2L})_{ab}$  (open symbols) from underdoped to overdoped Hg1212 [3]. Each dashed line indicates  $T_c$ . (d)  $T$  dependences of  $\Delta J_{cc}/\Delta J_{ab}$  [3]. (e) Phase diagram of Hg1212:  $T_c$  (closed circles), the pseudo spin-gap temperature defined by the maximum temperature of  $1/T_1 T$  [7] (closed squares),  $T_p$  defined by the peak temperature of  $(1/T_{2L})_{cc}$  [3] (open triangles) against hole concentration  $P_{sh}$ . The dotted curve with a shaded region is a visual guide for the onset temperature  $T^*$  of decrease in  $^{63}\text{Cu}$  Knight shift [7]. Nearly AF stands for the Curie-Weiss law in Cu  $1/T_1 T$  [7].

$1/T_1T$ ,  $T_p$  defined by the peak temperature of  $(1/T_{2L})_{cc}$ , and the onset temperature  $T^*$  of the decrease in the Cu Knight shift are plotted against the hole concentration  $P_{sh}$  in  $\text{Cu}^{2+P_{sh}}$  [3, 7]. With hole doping,  $T^*$  decreases, while  $T_p$  is nearly independent of the hole concentration  $P_{sh}$ . The ultraslow fluctuations emerge in the underdoped regime and diminish in the overdoped regime.

### 3.2. Local field fluctuations

Local field fluctuations of  $J_{ab}$  ( $B \perp c$  axis) and  $J_{cc}$  ( $B \parallel c$  axis) causing the nuclear spin relaxations of  $T_1$  and  $T_2$  are defined by

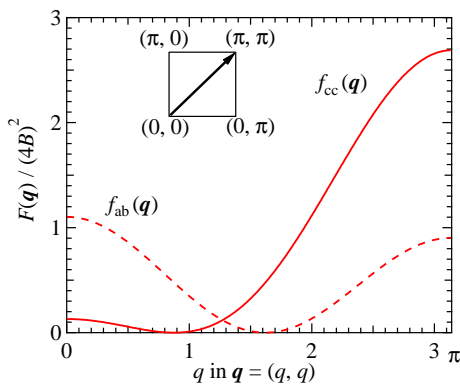
$$J_{\gamma\gamma} = \sum_{\mathbf{q}} F_{\gamma\gamma}(\mathbf{q}) S(\mathbf{q}, \nu_n), \quad (7)$$

$$F_{\gamma\gamma}(\mathbf{q}) \equiv (4B)^2 f_{\gamma\gamma}(\mathbf{q}) = [A_{\gamma\gamma} + 2B\{\cos(q_x) + \cos(q_y)\}]^2, \quad (8)$$

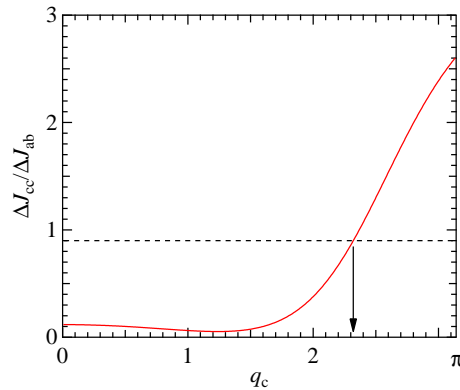
where  $\gamma\gamma = ab$  and  $cc$ , and  $\nu_n$  is an NMR frequency [3]. The electron spin-spin correlation function  $S(\mathbf{q}, \nu)$  (a frequency  $\nu$ ) is related to the dynamical spin susceptibility  $\chi''(\mathbf{q}, \nu)$  through the fluctuation-dissipation theorem.  $F_{\gamma\gamma}(\mathbf{q})$  is called the form factor of the wave vector  $\mathbf{q}$  dependent hyperfine coupling constant, whose filtering effects in the  $\mathbf{q}$  space play a significant role in the anisotropy and the site differentiation on NMR [8, 9, 10].  $\Delta J_{\gamma\gamma}$  expresses the additional fluctuations to  $J_{\gamma\gamma}$  [3].

Figure 5 shows the  $q$  dependence of  $f_{ab, cc}(\mathbf{q})$  for Hg1212 along the diagonal  $\mathbf{q} = (q, q)$  in the first Brillouin zone, using the estimated coupling constant ratios in Table 1. Since  $f_{cc}(\pi, \pi) > f_{ab}(\pi, \pi)$ , the antiferromagnetic spin fluctuation  $\chi'(\mathbf{q})$  localized around  $\mathbf{q} = [\pi, \pi]$  leads to the anisotropy  $J_{cc}/J_{ab} \sim 3$  in contrast to the experimental ratio  $\Delta J_{cc}/\Delta J_{ab} < 1$  in figure 4(d) [3].  $\Delta J_{\gamma\gamma}$  expresses the development of the ultraslow fluctuations [3]. Thus, the antiferromagnetic fluctuations are excluded from the ultraslow fluctuations.

Let us assume a toy model of  $\chi'(\mathbf{q}, \nu_n) = \chi'_0 \Theta(q_c - |q_x|) \Theta(q_c - |q_y|)$  ( $\Theta(x)$  is the Heaviside step function).  $q_c$  is a cut-off wave number.  $\chi'(\mathbf{q}) \propto S(\mathbf{q}, \nu_n)$  takes a constant value  $\chi'_0$  over



**Figure 5.**  $^{63}\text{Cu}$  hyperfine coupling form factors  $f_{cc}(\mathbf{q})$  and  $f_{ab}(\mathbf{q})$  as functions of  $q$  in the wave vector  $\mathbf{q} = (q, q)$   $[(0, 0) \rightarrow (\pi, \pi)]$ . Inset shows the diagonal in the first Brillouin zone.



**Figure 6.**  $\Delta J_{cc}/\Delta J_{ab}$  as a function of the cut off  $q_c$  in a toy model upon a static spin susceptibility  $\chi'(\mathbf{q}) = \chi'_0 (|q_{x,y}| < q_c)$  and 0 ( $|q_{x,y}| > q_c$ ). Experimental constraint leads to  $q_c < 2.3$ .

$|q_{x,y}| < q_c$ . For this toy model, the ratio  $\Delta J_{cc}/\Delta J_{ab}$  is calculated as

$$\frac{\Delta J_{cc}}{\Delta J_{ab}} = \frac{\sum_{|q_{x,y}| < q_c} f_{cc}(\mathbf{q})}{\sum_{|q_{x,y}| < q_c} f_{ab}(\mathbf{q})}. \quad (9)$$

Figure 6 shows the numerical  $\Delta J_{cc}/\Delta J_{ab}$  as a function of  $q_c$ . The experimental  $\Delta J_{cc}/\Delta J_{ab} < 0.9$  in figure 4(d) imposes on the function in figure 6 and then leads to  $q_c < 2.3$ . The magnetic ultraslow fluctuations must be confined within  $q_c < 2.3$ . If the magnetic ultraslow fluctuations have the easy plane anisotropy, the upper limit of the cut-off value  $q_c$  will be smaller than 2.3. Thus, we obtained a model constraint on the magnetic ultraslow fluctuations, using the anisotropic hyperfine coupling constants.

Although the step function  $\chi'(\mathbf{q})$  with  $q_c < 2.3$  is not localized at  $q = 0$ , it is parallel to the IUC  $q = 0$  magnetic moments observed by the spin polarized neutron scattering method [1]. The ultraslow fluctuations may be associated with the IUC  $q = 0$  magnetic moments. However, if the enhancement in  $1/T_{2L}$  is due to quadrupole fluctuations, one should explore the alternative fluctuations of charge or lattice for the electric ultraslow fluctuations.

#### 4. Conclusions

The systematic hole doping dependences of the  $^{63}\text{Cu}$  hyperfine coupling constants ( $A_{cc}$ ,  $A_{ab}$  and  $B$ ) were found for Hg1212 from underdoped to overdoped. A model constraint on the magnetic ultraslow fluctuations in Hg1212 was derived from the anisotropy ratios of the  $^{63}\text{Cu}$  hyperfine coupling constants. The model expresses the magnetic fluctuations spread around  $q = 0$ . Possible electric ultraslow fluctuations causing the  $T_2$  anomaly remain to be explored.

#### Acknowledgments

We thank Jun Kikuchi for fruitful discussions on the hyperfine coupling constants.

#### References

- [1] Bourges P and Sidis Y 2011 *C. R. Physique* **12** 461
- [2] Varma C M 2014 *J. Phys.: Condens. Matter* **26** 505701
- [3] Itoh Y, Machi T and Yamamoto A 2017 *Phys. Rev. B* **95** 094501
- [4] Singer P M, Hunt A W, Cederström A F and Imai T 1999 *Phys. Rev. B* **60** 15345
- [5] Hunt A W, Singer P M, Cederström A F and Imai T 2001 *Phys. Rev. B* **64** 134525
- [6] Mila F and Rice T M 1989 *Physica C* **157** 561
- [7] Itoh Y, Tokiwa-Yamamoto A, Machi T and Tanabe K 1998 *J. Phys. Soc. Jpn.* **67** 2212
- [8] Millis A J, Monien H and Pines D 1990 *Phys. Rev. B* **42** 167
- [9] Monien H, Pines D and Slichter C P 1990 *Phys. Rev. B* **41** 11120
- [10] Imai T 1990 *J. Phys. Soc. Jpn.* **59** 2508
- [11] Itoh Y, Hayashi A and Ueda Y 1995 *J. Phys. Soc. Jpn.* **64** 3074
- [12] Rybicki D, Kohlrautz J, Haase J, Greven M, Zhao X, Chan M K, Dorow C J and Veit M J 2015 *Phys. Rev. B* **92** 081115
- [13] Shimizu T, Aoki H, Yasuoka H, Tsuda T, Ueda Y, Yoshimura K and Kosuge K 1993 *J. Phys. Soc. Jpn.* **62** 3710
- [14] Hanzawa K 1994 *J. Phys. Soc. Jpn.* **63** 264
- [15] Okabe Y and Kikuchi M 1988 *J. Phys. Soc. Jpn.* **57** 4751
- [16] Terasaki I, Hase M, Maeda A, Uchinokura K, Kimura T, Kishio K, Tanaka I and Kojima H 1992 *Physica C* **193** 365
- [17] Haase J, Jurkutat M, Kohlrautz J 2017 *Condens. Matter* **2** 16
- [18] Takigawa M, Hammel P C, Heffner R H, Fisk Z, Smith J L and Schwarz R B 1989 *Phys. Rev. B* **39** 300
- [19] Pennington C H, Durand D J, Slichter C P, Rice J P, Bukowski E D and Ginsberg D M 1989 *Phys. Rev. B* **39** 2902
- [20] Bleaney B, Bowers K D and Pryce M H L 1955 *Proc. Roy. Soc. London, Ser. A* **228** 166
- [21] Hüsser P, Suter H U, Stoll E P and Meier P F 2000 *Phys. Rev. B* **61** 1567

- [22] Itoh M, Sugahara M, Yamauchi T and Ueda Y 1996 *Phys. Rev. B* **53** 11606
- [23] Itoh Y, Machi T and Yamamoto A [arXiv:2091155]
- [24] Itoh Y, Machi T, Adachi S, Fukuoka A, Tanabe K and Yasuoka H 1998 *J. Phys. Soc. Jpn.* **67** 312
- [25] Kitaoka Y, Fujiwara K, Ishida K, Asayama K, Shimakawa Y, Manako T and Kubo Y 1991 *Physica C* **179** 107
- [26] Kambe S, Yasuoka H, Hayashi A and Ueda Y 1993 *Phys. Rev. B* **47** 2825
- [27] Ishida K, Kitaoka Y, Asayama K, Kadowaki K and Mochiku T 1994 *J. Phys. Soc. Jpn.* **63** 1104
- [28] Shimizu S, Iwai S, Tabata S-I, Mukuda H, Kitaoka Y, Shirage P M, Kito H and Iyo A 2011 *Phys. Rev. B* **83** 144523
- [29] Huang N L, Orbach R, Šimánek E, Owen J and Taylor D R 1967 *Phys. Rev.* **156** 383



